Available online at www.sciencedirect.com

SCIENCE DIRECT

Biochimica et Biophysica Acta 1708 (2005) 238–249

BIOCHIMICA ET BIOPHYSICA ACTA
BBA

http://www.elsevier.com/locate/bba

EPR study of electron transport in the cyanobacterium *Synechocystis* sp. PCC 6803: Oxygen-dependent interrelations between photosynthetic and respiratory electron transport chains

Boris V. Trubitsin[a], Vasilii V. Ptushenko[a], Olga A. Koksharova[b], Mahir D. Mamedov[b], Liya A. Vitukhnovskaya[b], Igor A. Grigor'ev[c], Alexey Yu. Semenov[b], Alexander N. Tikhonov[a,*]

[a]*Department of Biophysics, Faculty of Physics, M.V. Lomonosov Moscow State University, Moscow 119992, Russia*
[b]*A.N.Belozersky Institute of Physico-Chemical Biology, M.V. Lomonosov Moscow State University, Moscow 119992, Russia*
[c]*Institute of Organic Chemistry, Novosibirsk, Russia*

Received 18 January 2005; received in revised form 18 February 2005; accepted 8 March 2005
Available online 24 March 2005

Abstract

In this work, we investigated electron transport processes in the cyanobacterium *Synechocystis* sp. PCC 6803, with a special emphasis focused on oxygen-dependent interrelations between photosynthetic and respiratory electron transport chains. Redox transients of the photosystem I primary donor P700 and oxygen exchange processes were measured by the EPR method under the same experimental conditions. To discriminate between the factors controlling electron flow through photosynthetic and respiratory electron transport chains, we compared the P700 redox transients and oxygen exchange processes in wild type cells and mutants with impaired photosystem II and terminal oxidases (*Cta*I, *Cyd*AB, *Cta*DEII). It was shown that the rates of electron flow through both photosynthetic and respiratory electron transport chains strongly depended on the transmembrane proton gradient and oxygen concentration in cell suspension. Electron transport through photosystem I was controlled by two main mechanisms: (i) oxygen-dependent acceleration of electron transfer from photosystem I to $NADP^+$, and (ii) slowing down of electron flow between photosystem II and photosystem I governed by the intrathylakoid pH. Inhibitor analysis of P700 redox transients led us to the conclusion that electron fluxes from dehydrogenases and from cyclic electron transport pathway comprise 20–30% of the total electron flux from the intersystem electron transport chain to $P700^+$.

Keywords: Cyanobacteria; Electron transport control; Electron paramagnetic resonance

1. Introduction

The structural and functional organization of the photosynthetic systems of higher plant chloroplasts and cyanobacteria is known sufficiently well. The main achievements in this field include determination of the sequence of the light and dark stages of photosynthesis and clarification of molecular mechanisms of key reactions of electron and proton transport in chloroplasts (see Ref. [1] for review). Elucidation of regulatory mechanisms of electron transport processes in native photosynthetic systems and their adaptation to variable environmental conditions are central problems in bioenergetics of photosynthesis [2–4]. There

Abbreviations: PS I and PS II, Photosystem I and photosystem II, respectively; P700, primary electron donor of photosystem I; PQ, plastoquinone; PQH_2, plastoquinol; NDH-1, type I NADPH dehydrogenase; SDH, succinate dehydrogenase; Cyt, cytochrome; EPR, electron paramagnetic resonance; DCMU, 3-(3,4-dichloro-phenyl)-1, 1-dimethylurea; DBMIB, 2,5-dibromo-3-methyl-6-isopropyl-*p*-benzoquinone; CCCP, carbonylcyanide-3-chlorophenyl hydrazone; TCPO, 2,2,5,5-tetramethyl-3-carboxy-pyrroline-1-oxyl; WT, wild type; Ox^-, oxidase-deficient mutant

* Corresponding author. Tel.: +7 095 9392973; fax: +7 095 9328820.
E-mail address: an_tikhonov@newmail.ru (A.N. Tikhonov).

0005-2728/$ - see front matter © 2005 Elsevier B.V. All rights reserved.
doi:10.1016/j.bbabio.2005.03.004

are different mechanisms of regulation of photosynthetic processes, which may include: (i) electron transport control on the donor side of photosystem I (PS I) due to slowing down of plastoquinol (PQH_2) oxidation caused by acidification of the intrathylakoid lumen [5–8]; (ii) acceleration of electron efflux from PS I due to the light-induced activation of the Calvin cycle enzymes [9]; (iii) state 1↔ state 2 transitions associated with redistribution of light energy between PS I and PS II, which are controlled by the redox state of electron carriers between PS I and PS II [10]; (iv) redox-controlled switching of electron transport pathways between noncyclic (PS I→$NADP^+$), pseudocyclic (H_2O→H_2O cycle) and cyclic electron flow around PS I [11,12]; (v) oxygen-dependent switching between photosynthetic and respiratory pathways of plastoquinol oxidation; (vi) energy-dependent regulation of carbon concentrating mechanisms [13]; and (vii) regulation of photosynthetic processes at the level of gene expression [14].

Investigation of oxygen-dependent interrelations between photosynthetic and respiratory electron transport chains in oxygenic photosynthetic organisms is yet another important and interesting field of research [15]. The cyanobacterium *Synechocystis* sp. PCC 6803 is an excellent model for in vivo studies of regulation of bioenergetic processes in photosynthetic organism of oxygenic type [16,17]. Cyanobacteria contain both oxygenic photosynthetic and respiratory electron transfer chains incorporated into the same membrane. *Synechocystis* sp. PCC 6803 is the first photosynthetic organism with completely sequenced genome [18]. The X-ray crystal structures of the PS I, PS II and cytochrome (cyt) *bf*-complex have been recently resolved in *Synechococcus elongatus* and other thermophilic cyanobacteria [19–23].

In this work, in order to elucidate the role of oxygen-dependent interrelations between photosynthetic and respiratory electron transport chains in regulation of electron transport in intact cyanobacteria cells, we studied the influence of pre-illumination conditions on the kinetics of light-induced redox transients of P700 in *Synechocystis* sp. PCC 6803 (some preliminary results were published in [24]). Kinetic behavior of PS I primary donor (P700) was compared with the oxygen exchange processes measured under similar conditions by the EPR method. Our attention was focused on the regulatory processes in two checkpoints of photosynthetic electron transport, on the donor and acceptor sides of PS I. It was shown that the rates of electron flow through both photosynthetic and respiratory electron transport chains in the intact cyanobacteria *Synechocystis* sp. PCC 6803 depended on the membrane energization and oxygen concentration in cell suspension. We conclude that photosynthetic electron transport is controlled by two main mechanisms: (i) oxygen-dependent acceleration of electron transfer from PS I, and (ii) slowing down of electron flow between PS II and PS I governed by the intrathylakoid pH.

2. Materials and methods

2.1. Strains and growth conditions

Wild type *Synechocystis* sp. PCC 6803 cells were grown in BG-11 medium [25] as described earlier [24]. Liquid cultures were grown at 30 °C under continuous white fluorescence illumination (~100 $\mu E \cdot m^{-2}s^{-1}$); cultures were bubbled with atmospheric air without supplemented CO_2. We used two mutant strains: terminal oxidase-less (Ox^-) mutant (*Cta*I, *Cyd*AB, *Cta*DEII) [26] and PS II-less ($PS\ II^-$) mutant [27]. Strains of *Synechocystis* sp. PCC 6803 mutant cells were a gift from Dr. W.F.J. Vermaas (USA). Mutant cells were cultivated for 7–10 days in air at 30 °C in BG-11 medium under aerobic conditions in Erlenmeyer flasks, either photoautotrophically (Ox^-) or with 5 mM glucose ($PS\ II^-$). For growth on plates, 1.5% (w/v) agar was added, and BG-11 was supplemented with antibiotics appropriate for the particular strain (25 $\mu g\ ml^{-1}$ kanamycin, 25 $\mu g\ ml^{-1}$ erythromycin and 25 $\mu g\ ml^{-1}$ spectinomycin). Cells from liquid cultures were harvested by centrifugation, washed once with 10 mM Tris–HCl buffer (pH 7.5) at a Chl concentration 0.6–1 mg ml^{-1}, and used directly for measurements.

2.2. Preparations of PS I complex

PS I complexes were isolated from the wild type *Synechocystis* sp. PCC strain 6803 cells as described elsewhere [28].

2.3. EPR measurements of P700 turnover

EPR spectra were measured with a Varian E-4 X-band spectrometer. Samples were placed either in an oxygen-permeable plastic tube (TFE tubes from Zeus Inc.; internal diameter, 0.635 mm; wall thickness, 0.051 mm) or in a standard flat quartz cuvette (internal thickness, 0.1 mm) positioned in the cavity of the EPR spectrometer. Cells were illuminated with subsaturating white light from a 100 W tungsten lamp (~10 mE $m^{-2}s^{-1}$ at the sample surface); infrared light was cut off with a 5-cm layer of water. Usually, EPR signals from oxidized reaction centers $P700^+$ were recorded at 22 °C at subsaturating microwave power 10 mW and modulation amplitude 4 G. For measuring the kinetics of the light-induced redox transients of P700, magnetic field was fixed, as a rule, at the low-field extremum of the EPR signal from $P700^+$. In order to avoid potential artifacts that might appear due to the EPR signals from other species, we performed additional measurements: (i) kinetic behavior of P700 was measured by fixing magnetic field at the hight-field peak of the EPR signal from $P700^+$, and (ii) EPR spectra were recorded at relatively low modulation amplitude (0.4 G), at which the superfine structure of organic radicals (e.g., semiquinone radicals of 2,5-dibromo-3-methyl-6-isopropyl-*p*-benzoqui-

none (DBMIB) or ascorbic acid) becomes well-resolved. In most experiments, kinetic curves were recorded using the time constant 0.3 s. To measure the post-illumination kinetics of $P700^+$ reduction, the continuous light was abruptly cut off with a mechanical shutter (actuation time, <0.8 ms). To resolve relatively fast kinetics of $P700^+$ reduction, the EPR signal decay was recorded with the resolution time ~1 ms. In this case, the signal-to-noise ratio was improved by averaging several kinetic curves (up to 70–90 light–dark cycles separated by 1 min dark intervals). In order to bring the experimental conditions to a standard level, we used either of the following two protocols. According to the first protocol, an aerated aliquot from the cell suspension was placed in an EPR cell and then adapted to the dark for 10 min before switching-on the light (so-called "dark-adapted" cells). According to the second protocol, each sample was preliminarily illuminated for 1 min with white light and then adapted to the dark for a certain interval of time. Concentration of P700 in cell suspensions used for EPR measurements was ~5–10 μM.

2.4. EPR oximetry

As a probe for oxygen evolution/uptake by cyanobacteria, we used a spin label 2,2,5,5-tetramethyl-3-carboxy-pyrroline-1-oxyl (TCPO). By measuring the EPR spectra of the oxygen-sensitive spin label TCPO dissolved in cell suspension, we were able to monitor the uptake or evolution of oxygen under virtually the similar experimental conditions as those used to monitor the light-induced kinetics of P700 redox transients. The concentration of TCPO in the cell suspension was 0.1 mM. EPR spectra of TCPO were measured at microwave power 10 mW and modulation amplitude 0.05 G.

2.5. Reagents

All reagents used for preparing cell cultivation media and buffer solutions were purchased from Sigma. Spin label TCPO was synthesized as described earlier [29]. Stock solutions of carbonylcyanide-3-chlorophenyl hydrazone (CCCP), 3-(3,4-dichloro-phenyl)-1, 1-dimethylurea (DCMU), and DBMIB from Sigma were prepared in double-distilled ethanol. The concentrations of ethanol added to samples never exceeded 1%. This amount of ethanol did not influence the kinetics of P700 redox transients or oxygen exchange.

3. Results

3.1. EPR spectra

Fig. 1A demonstrates EPR signals from wild type *Synechocystis* sp. PCC 6803 cells. In the dark, cyanobacterial cells showed the EPR signal with the following spectral

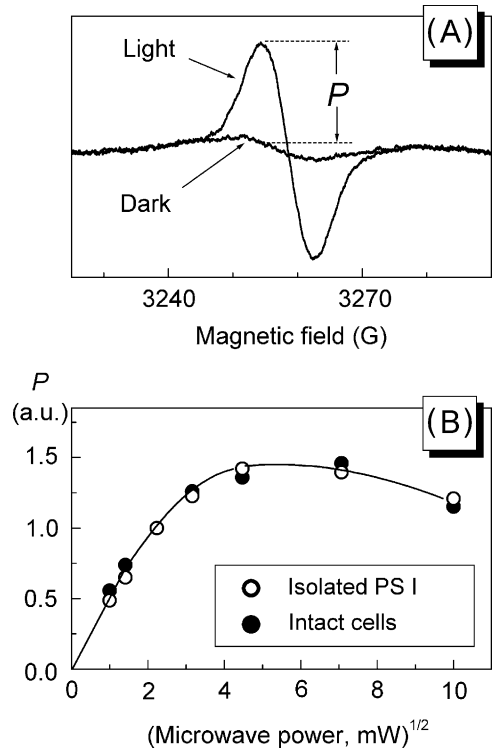

Fig. 1. (A) EPR spectra of wild type *Synechocystis* sp. PCC 6803 cells in the dark and during illumination. (B) Dependence of the normalized amplitude P of the light-induced EPR signal from $P700^+$ in isolated PS I complex and intact cells on the microwave power.

parameters $\Delta H_{pp}=16$ G and $g=2.0045$, which could be attributed to tyrosine radicals in PS II complex [30]. Illumination of cells with continuous white light induced the EPR signal that was typical of oxidized centers $P700^+$ [31]. The spectral parameters of this signal ($\Delta H_{pp}=8$ G, $g=2.0025$) were the same as those given by isolated PS I complex (not shown). Fig. 1B shows that the light-induced EPR signals in intact cells and in isolated PS I complexes have virtually the same dependencies of the signal amplitude on the microwave power, indicating that relaxation characteristics of these signals are the same. These observations (the coincidence of spectral and relaxation characteristics of the EPR signals) are evidence of the identity of the light-induced EPR signal observed in intact cells with the EPR signal from $P700^+$.

3.2. Kinetics of light-induced oxidation of P700

Fig. 2 shows the typical patterns of the light-induced changes in the height of the EPR signal from $P700^+$ in suspension of dark-adapted cells *Synechocystis* sp. PCC 6803 (wild type). Switching continuous light on caused oxidation of P700. Kinetics of this process strongly depended on the illumination prehistory (duration of dark interval before illumination) and conditions of cell incubation, i.e., either a suspension of cells was placed in a gas-impermeable quartz cuvette (Fig. 2A) or in a gas-permeable plastic TFE tube (Fig. 2B).

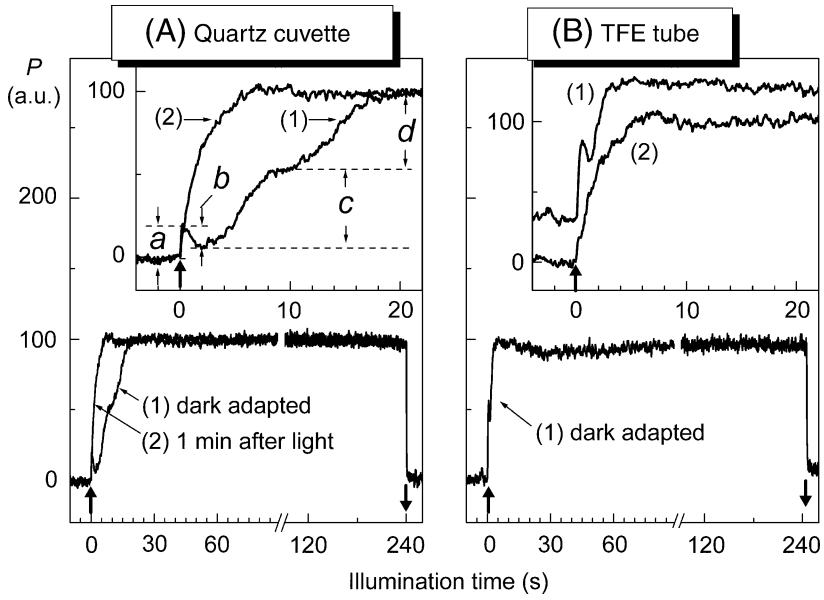

Fig. 2. Kinetics of the light-induced changes in the amplitude of the EPR signal from $P700^+$ in wild type *Synechocystis* sp. PCC 6803 cells incubated in quartz cuvette (A) or plastic TFE tube (B). Before switching the light on, cells were adapted to the dark either for 10 min (curves 1, adaptation of cells without pre-illumination) or for 1 min (curves 2, adaptation of cells after illumination for 4 min). Note different time scales in top and bottom panels. Here and below, upward and downward arrows indicate switching the light on and off.

For dark-adapted cells placed in a gas-impermeable quartz cuvette (protocol 1, cells without pre-illumination, dark adaptation for 10 min inside cuvette), we observed a multiphase kinetics of the P700 redox transients (Fig. 2A, curve 1). Immediately after the light had been switched on, there was a relatively fast initial jump of the EPR signal (phase *a*, ≈15–20% of the total signal) followed by a certain decay (phase *b*) and subsequent relatively slow rise of the EPR signal up to a steady-state level (phases *c* and *d*, see top panel in Fig. 2A, curve 1). After turning off the light, the EPR signal decayed to the initial level (bottom panels in Fig. 2). Another pattern of P700 oxidation was observed after relatively short (1 min) adaptation of illuminated cells to the dark (Fig. 2A, curve 2). In this case, the light-induced oxidation of P700 was faster than in dark adapted cells. The retardation of P700 oxidation after sufficiently long dark adaptation (t_{ad} ≈ 10 min) can be explained by oxygen deprivation inside a quartz cuvette due to efficient respiration of cells [24]. Indeed, the light-induced oxidation of P700 in cells incubated inside a gas-permeable TFE tube (Fig. 2B) was much faster than in cells confined to a quartz cuvette (Fig. 2A).

For cells incubated under aerobic conditions, the kinetics of P700 oxidation also depended on the dark adaptation time (Fig. 2B). It should be noted, however, that the difference between the time-courses of P700 oxidation in aerated cyanobacteria (curves 1 and 2 in Fig. 2B) was not as dramatic as that observed in cells incubated in a quartz cuvette (curves 1 and 2 in Fig. 2A). Illumination of dark-adapted cells (t_{ad}=10 min) caused non-monotonous redox transients of P700. After initial relatively fast rise of the EPR signal from $P700^+$(≈ 40–60% of the total signal, depending on cyanobacteria preparation), we observed a small dip followed by a rapid elevation of the signal to a steady-state level (Fig. 2B, top panel, curve 1). After relatively short adaptation (≈ 1 min of darkness after illumination), we observed the monotonous kinetics of P700 oxidation (Fig. 2B, top panel, curve 2). The dependence of P700 redox transients on the duration of dark adaptation before illumination can be associated with changes in the redox state of electron transport chain and related regulatory phenomena (so-called "state 1 ↔ state 2" transitions [4,10]).

A substantial difference between the kinetic patterns of P700 oxidation in cells incubated in a quartz cuvette (Fig. 2A) or placed in a TFE tube (Fig. 2B) is accounted for by oxygen deprivation inside a quartz cuvette due to terminal oxidases found in both thylakoid and cytoplasm membranes of *Synechocystis* sp. PCC 6803 (see Refs. [16,17] for review). According to Ref. [24], the efflux of electrons from the acceptor side of PS I is decelerated under the oxygen deficit, whereas electron flow from plastoquinol (PQH_2) to $P700^+$ (via the cyt *bf*-complex and cyt c_6) is maintained at a high level due to over-reduction of the plastoquinone pool. For this reason, cells incubated in a gas-impermeable quartz cuvette show a relatively low level of $P700^+$ during first few seconds after switching the light on. With the light-induced regeneration of oxygen by the water splitting complex, the efflux of electrons from PS I becomes more efficient, thereby promoting the rise of the EPR signal from $P700^+$ (Fig. 2A). A correlation between the rate of P700 oxidation and the light-induced evolution of oxygen was confirmed in our experiments with the oxygen-sensitive spin label TCPO (results of these experiments are described below).

It should be noted that the adaptation effects outlined above cannot be explained by mere depletion of $NADP^+$ or CO_2. Actually, the slowing down of the light-induced oxidation of P700 was observed after adaptation of cells to the dark, provided that O_2 (but not CO_2) molecules were consumed by the respiratory chains. In the meantime, the illumination of dark-adapted cells for several minutes (when the concentration of CO_2 in cell suspension decreased and, therefore, the ratio $NADPH/NADP^+$ increased) did not cause any significant decrease in the steady-state level of $P700^+$ (Fig. 2). Moreover, the addition of excess amounts of inorganic carbon (HCO_3^-) to suspension medium (up to 50 mM) did not affect the light-induced signal from $P700^+$ (data not shown).

3.3. Effects of DCMU and DBMIB

There are several sources of electrons available for $P700^+$ reduction. In addition to PS II, electrons injected into the intersystem chain of electron transfer can be derived from dehydrogenases (type I NADPH dehydrogenase (NDH-1) and succinate dehydrogenase (SDH)) and from the acceptor side of PS I (via cyclic pathway of electron flow around PS I). To evaluate the contribution of these pathways to $P700^+$ reduction, we compared the kinetic behavior of P700 in cells treated with DBMIB and DCMU (Fig. 3). DBMIB is an inhibitor of the electron flow via cyt *bf*-complex; in the presence of DCMU, which inhibits PS II, electrons available for $P700^+$ reduction (via cyt *bf*-complex, cyt c_6/or plastocyanin) can be derived from dehydrogenases (NDH-1 and SDH) and/or from cyclic electron pathway around PS I.

In the presence of sufficient amounts of DBMIB (100 μM), which prevented electron flow from the plastoquinone pool to the cyt *bf*-complex, we observed monotonous kinetics of P700 oxidation (half-time ≈ 0.2 s), which were independent of cell incubation conditions, i.e. either in a quartz cuvette (Fig. 3A) or a plastic TFE tube (Fig. 3B). In contrast to DBMIB-treated cells, kinetics of P700 oxidation in DCMU-treated cells was sensitive to the incubation conditions. Under anaerobic conditions (Fig. 3A), the light-induced oxidation of P700 in DCMU-treated cells occurred significantly slower than in DBMIB-treated cells. This observation clearly demonstrates that during dark adaptation of cyanobacteria electron equivalents available for $P700^+$ reduction were accumulated in the intersystem electron transport chain. On the other hand, in DCMU-treated cells incubated under aerobic conditions (Fig. 3B), kinetics of P700 oxidation was similar to that observed in DBMIB-treated cells. This result shows that under aerobic conditions the plastoquinone pool in dark-adapted cells is maintained predominantly in the oxidized state. Thus, it is safe to conclude that under aerobic conditions, the plastoquinone pool reduced by dehydrogenases becomes re-oxidized by molecular oxygen through efficiently operating terminal oxidases.

Note that a steady state level of $P700^+$ established during illumination of DCMU-treated cells was somewhat smaller than in DBMIB-treated cells (Fig. 3). This difference is explained by $P700^+$ reduction by electrons available from dehydrogenases and from cyclic electron transport pathways (via the plastoquinone pool, cyt *bf*-complex, cyt c_6/or plastocyanin). It is easy to demonstrate that a steady state influx of electrons to $P700^+$ during cell illumination can be evaluated as $J_{in}=k_1A(1-p)$, where k_1 is the coefficient of proportionality determined by the intensity of light quanta delivered to P700, A is the steady state concentration of

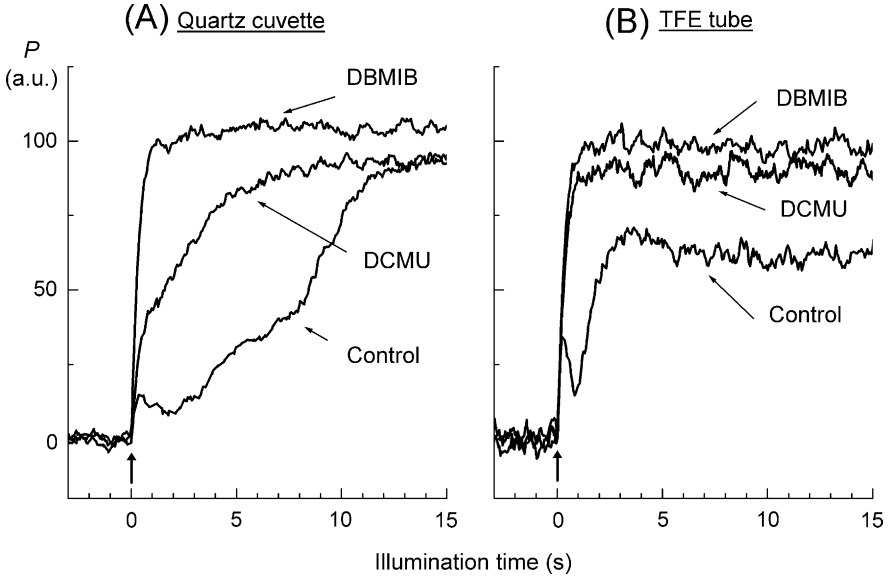

Fig. 3. Effects of inhibitors of electron transfer DCMU (100 μM) and DBMIB (100 μM) on the kinetics of the light-induced oxidation of P700 in wild type cells. Before EPR measurements, cells were adapted to the dark for 10 min (without pre-illumination) in quartz cuvette (A) or plastic TFE tube (B). Note that the effects caused by 100 μM DCMU or 100 μM DBMIB were complete, because the patterns of P700 redox transients remained unchanged with a further rise of the inhibitor concentrations.

oxidized electron acceptors on the acceptor side of PS I, and p is the relative number of oxidized centers $P700^+$. Assuming that under aerobic conditions the rates of electron outflow from the acceptor side of PS I are the same in DCMU-treated and in control cells (in this case the corresponding products k_1A should be the same), we can evaluate a relative contribution of dehydrogenases and cyclic electron transport chain to the overall electron donor pool available for $P700^+$ reduction. According to our data presented in Fig. 3B, these electron fluxes comprise 20–30% of the total electron flux from the intersystem electron transport chain to $P700^+$.

3.4. Effect of uncoupler CCCP on P700 redox transients

As shown in our previous work [24], the photosynthetic electron transport in *Synechocystis* sp. PCC 6803 was affected by uncouplers. By analogy with higher plant chloroplasts [5–8], we suggested that the light-induced acidification of the thylakoid lumen in cyanobacterium cell should cause the slowing down of PQH_2 oxidation by the cyt *bf*-complex (effect of photosynthetic control). This reaction is known to be the rate-liming step in the chain of electron transfer between two photosystems [1]. The results of our experiments with the uncoupler CCCP, which eliminates the transmembrane proton gradient ($\Delta\mu_{H^+}$) across the thylakoid membrane, substantiated this suggestion (Fig. 4). When cells were incubated inside a quartz cuvette in the presence of CCCP (Fig. 4A), the light-induced oxidation of P700 was markedly slower than in control samples. Under aerobic conditions (Fig. 4B, cells inside a plastic TFE tube), the rise of the EPR signal after dark adaptation was also affected by CCCP. In the presence of CCCP, kinetics of P700 oxidation displayed two phases—the fast one (similar to untreated cells) and the slower one—elevation of $P700^+$ to the steady state level.

The influence of CCCP on the kinetics of P700 oxidation can be explained, at least partially, by the release of electron transport control due to dissipation of $\Delta\mu_{H^+}$ by CCCP, i.e., due to acceleration of photosynthetic and respiratory electron transfer. Similarly to higher plant chloroplasts [5–8], the acidification of the thylakoid lumen in cyanobacteria should lead to the slowing down of the rate of PQH_2 oxidation by the cyt *bf*-complex. The rate of this process can be determined from the kinetics of $P700^+$ reduction after turning the light off [5–7]. Fig. 4C shows that in aerated sample the post-illumination reduction of $P700^+$ obeys the exponential law with the half-time $\tau_{1/2} \approx 55$ ms. In the presence of CCCP, the reduction of $P700^+$ was found to be almost two times faster ($\tau_{1/2} \approx 25$ ms), indicating that dissipation of $\Delta\mu_{H^+}$ by CCCP was accompanied by acceleration of electron flow to $P700^+$. This result clearly demonstrates that the rate of electron transfer between two photosystems depends on the membrane energization. In addition, CCCP may affect the kinetics of P700 oxidation, because it is an inhibitor of the oxygen-evolving activity of PS II complex [32]. The loss of PS II activity, which should cause slowing down of oxygen evolution and electron donation to the PQ pool, may affect the rates of the electron flow on the acceptor and donor sides of PS I.

3.5. Spin label oximetry

The necessity of oxygen for normal functioning of cyanobacteria was confirmed in experiments with a spin label TCPO used as an oxygen sensor. Fig. 5A shows the

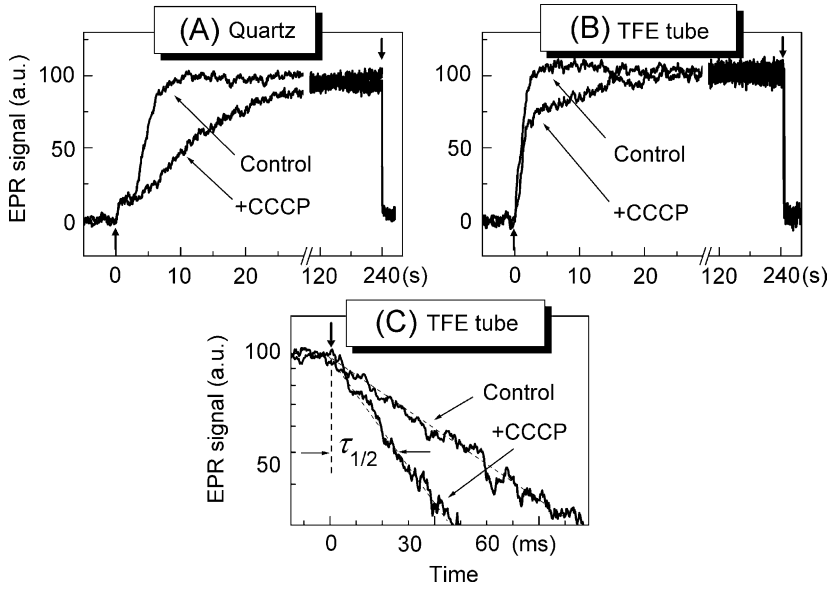

Fig. 4. Effects of CCCP (80 μM) on the kinetics of the light-induced changes in the amplitude of the EPR signal from $P700^+$ in dark-adapted cells in quartz cuvette (A) or plastic TFE tube (B). Before EPR measurements, cells were pre-illuminated for 4 min and then adapted to the dark for 10 minutes. (C) Semilogarithmic plot of the kinetics of $P700^+$ reduction in the dark after 1-min illumination of cells incubated in plastic TFE tube.

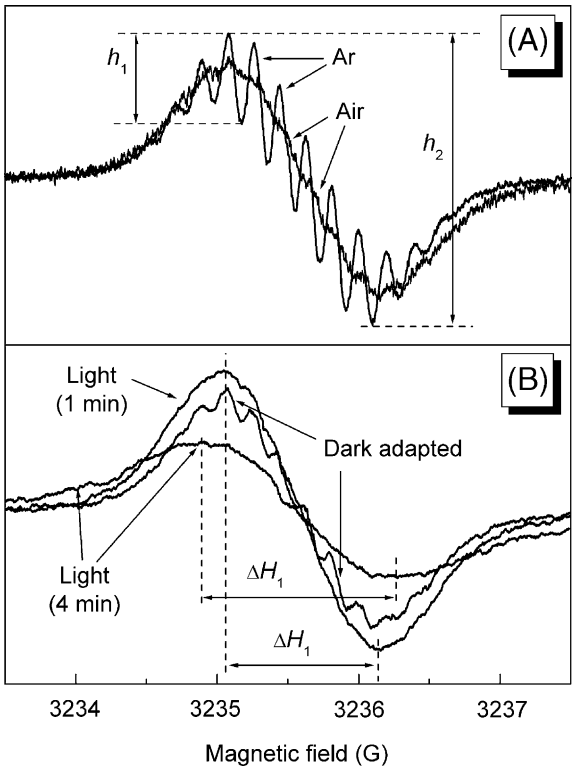

Fig. 5. The low-field components of the EPR signals from TCPO in water (A) and in cell suspension (B).

low-field components of the EPR signals from TCPO dissolved in aerated or deoxygenated water solutions, as indicated. In deoxygenated water (TCPO solution bubbled with Ar for 20 min), the spectral line had a well resolved superhyperfine structure (multiplet) arising due to interaction of the unpaired electron with the protons of the TCPO molecule. In aerated water solution, the multiplet was unresolved. The disappearance of the well resolved superhyperfine structure is explained by line broadening due to TCPO collisions with paramagnetic O_2 molecules. Following the previous works [33–35], we took the spectral parameter $\alpha = h_1/h_2$ (see definitions in Fig. 5A), which could be used as a measure for monitoring the oxygen consumption in water solutions of TCPO.

Fig. 5B demonstrates that after incubation of cyanobacteria in the dark in a quartz cuvette for 10 min, the EPR signal of TCPO acquired a well resolved superhyperfine structure, indicating a depletion of oxygen in a cell suspension. The illumination of cells caused a smoothing of the multiplet structure due to the light-induced recovery of oxygen. After sufficiently high oxygenation of cell suspension, when collisions of spin labels with O_2 molecules became more frequent, the multiplet transformed into a single line without the superhyperfine structure (Fig. 5B, illumination for 1 min). According to our calibration curve (parameter α vs. $[O_2]$, data not shown), in aerated suspension ($[O_2] > 150-240$ μM) parameter α cannot anymore be used as a measure of oxygen concentration. In this case, however, a spectral line can be characterized by the peak-to-peak linewidth ΔH_{pp} (Fig. 5B), which increases with the rise of oxygen concentration (compare spectral lines corresponding to 1 and 4 min of cell illumination).

3.6. Kinetics of oxygen exchange

Fig. 6 compares the typical patterns of the time-courses of oxygen-sensitive parameters α (top boxes) and ΔH_{pp} (bottom boxes) for spin probe TCPO in suspensions of wild type (WT) and oxidase-deficient (Ox^-) mutant of *Synecho-*

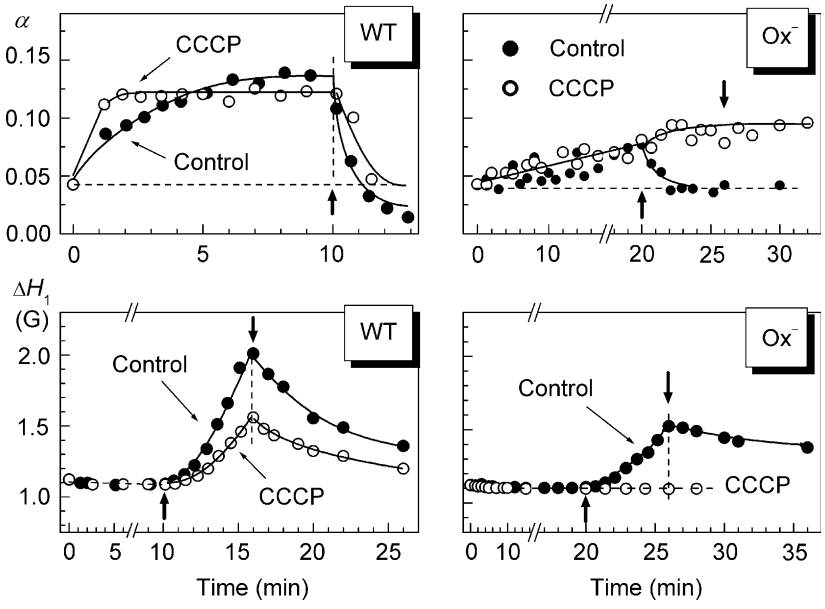

Fig. 6. Effects of CCCP (80 μM) on the kinetics of the light-induced changes in spectral parameters α and ΔH_1 of the low-field components of the EPR signals from TCPO in wild type (WT) and oxidase deficient (Ox^-) mutant of *Synechocystis* sp. PCC 6803. Before the EPR measurements, each sample was aerated by stirring and then placed in quartz cuvette. Upward and downward arrows indicate switching the light on and off.

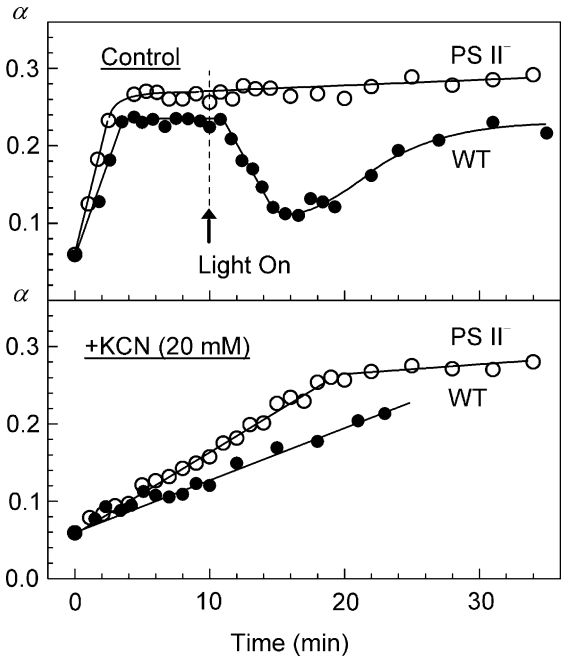

Fig. 7. Effect of KCN on the time-courses of the spectral parameter α of the low-field components of the EPR signals from TCPO in glycerol-treated wild type (WT) cells and in PS II deficient (PS II⁻) mutant of *Synechocystis* sp. PCC 6803. Before the EPR measurements, each sample was aerated by stirring and then placed in quartz cuvette.

cystis sp. PCC 6803. In these experiments, aerated samples were placed into a gas-impermeable quartz cuvette and then EPR spectra of TCPO were recorded step-by-step. For WT cells, we observed a relatively fast increase in the spectral parameter α up to the steady-state level of ≈ 0.12 (Fig. 6, left top box), which reflected the oxygen consumption by cells in the dark (up to $[O_2] \leq 20–25$ μM). In the presence of CCCP, the rate of oxygen uptake in the dark accelerated by a factor of 2–3, demonstrating that electron transport through respiratory chain from dehydrogenases to molecular oxygen was controlled by the proton electrochemical potential. After the light had been switched on, parameter α rapidly decreased due to the light-induced regeneration of oxygen by PS II. The decrease in α was observed in parallel with the light-induced rise of the linewidth ΔH_{pp} (Fig. 6, left bottom box). According to our calibration curve (ΔH_{pp} vs. $[O_2]$, data not shown), a substantial increase in ΔH_{pp} observed after sufficiently long illumination of cells demonstrates that the concentration of oxygen inside quartz cuvette goes above 400 μM. In the presence of CCCP, the rate of the light-induced evolution of oxygen declined. This could be explained, at least partly, by a certain suppression of water-splitting processes by CCCP, which is known as an ADRY-agent impairing the PS II activity [32]. In case of the Ox⁻ mutant, the rate of respiration in darkness (Fig. 6, right top box) was negligible as compared to the WT cells. Although illumination of Ox⁻ cells caused evolution of oxygen, the rate of this process (Fig. 6, right bottom box) was markedly slower than in the WT cells. It is noteworthy that CCCP completely suppressed the light-induced production of oxygen by mutant cells. One of explanations of this result is that in the Ox⁻ mutant the PSII complex is less resistant to the action of CCCP than in WT cells.

Fig. 7 compares the kinetic behavior of the oxygen-sensitive parameter α measured in suspensions of WT and PS II-deficient (PS II⁻) mutant cells placed in quartz cuvettes. In both cases, we observed relatively fast consumption of oxygen in the dark (Fig. 7A). However, in contrast to WT cells, PS II⁻ mutant cells were unable to evolve oxygen during illumination. The addition of DCMU, an inhibitor of PS II, also suppressed the light-induced evolution of oxygen by WT cells (data not shown). In the presence of 20 mM KCN, which should completely inhibit cyanide-sensitive terminal oxidases, the rates of oxygen consumption by both WT and PS II⁻ cells (Fig. 7B) were slowed down by a factor of 6. Remaining respiration could be assigned to KCN−resistant oxidases and/or to so-called chlororespiration process [36].

3.7. Correlation between the light-induced evolution of oxygen and P700 oxidation

For convincing demonstration of a close relationship between the oxygen evolution and kinetics of P700 redox

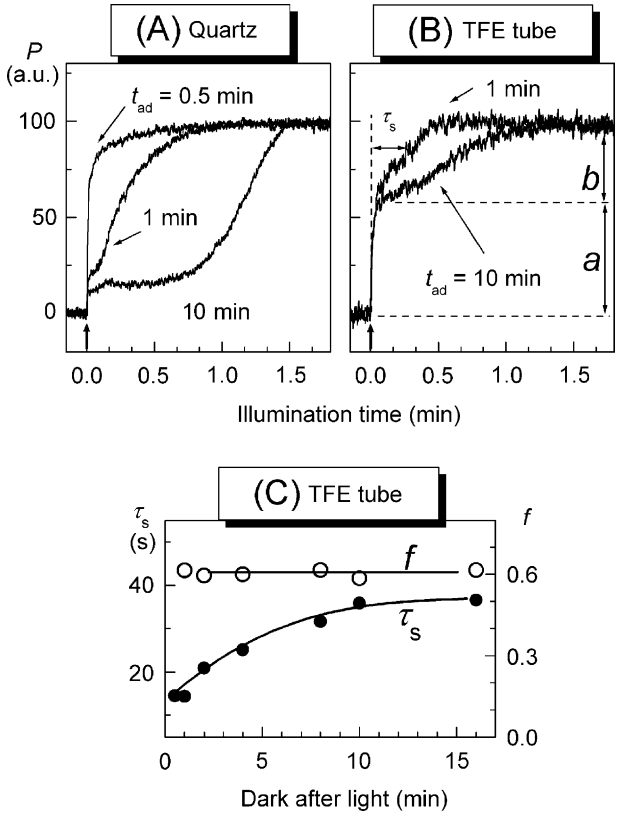

Fig. 8. Effects of dark adaptation on the light-induced oxidation of P700 in glycerol-treated wild type cells incubated in quartz cuvette (A) or plastic TFE tube (B, C). Before switching the light on, cells were pre-illuminated for 4 min and then adapted to the dark either for t_{ad}=0.5, 1 or 10 min, as indicated. (C) Dependence of the slow phase *b* parameters τ_s and $f=b/(a+b)$ on the dark adaptation time t_{ad}.

transients, we consider below these processes in glycerol-treated cells. Glycerol-treated cells are characterized by much lower rates of oxygen evolution and P700 oxidation as compared to untreated cells. This circumstance allows comparing the kinetics of P700 redox transients and oxygen exchange measured under similar experimental conditions by the EPR method. Fig. 8 demonstrates the typical patterns of P700 redox transients in the samples that were stored frozen (at 77 K in the presence of 20% glycerol used as a cryoprotector) before EPR measurements. Nevertheless, the influence of pre-illumination history on the kinetic behavior of P700 in glycerol-treated cells (Fig. 8) was similar, in general, to that observed in untreated samples (Fig. 2). For cells placed in a gas-impermeable quartz cuvette (Fig. 8A), the time-course of P700 oxidation slowed down substantially with increasing dark adaptation time. Under aerobic conditions (Fig. 8B), the ratio between the amplitudes of fast (a) and slow (b) phases of P700 oxidation was virtually independent of dark adaptation, whereas the half-time τ_s of the slow phase (see Fig. 8B for definition) increased with the adaptation time (Fig. 8C). Characteristic times of approaching the steady state level of $P700^+$ in glycerol-treated cells (Fig. 8A) were significantly longer than in "intact" samples (Fig. 2A). It should be noted that this effect was caused by the addition of glycerol rather than due to the freezing/thawing procedure (data not shown). The effect of glycerol could be explained, for instance, by its influence on the structural organization of the light-harvesting antenna [37] and electron transport protein complexes.

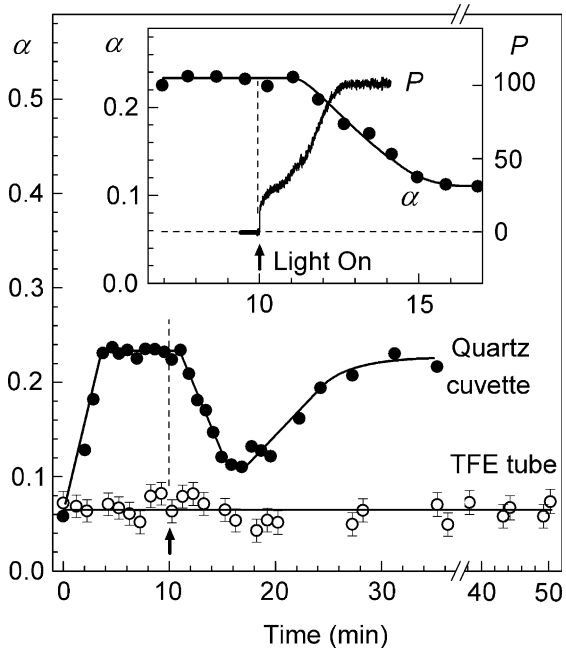

Fig. 9. Time-courses of the spectral parameter α of the low-field components of the EPR signals from TCPO in glycerol-treated wild type cells placed either in quartz cuvette or plastic TFE tube, as indicated. The insert box shows a correlation between the kinetics of the light-induced oxidation of P700 (parameter *P*) and oxygen evolution (parameter α).

Fig. 9 compares the time-courses of the oxygen-sensitive parameter α and P700 redox transients in glycerol-treated cells. For cells placed in a plastic TFE tube, the concentration of oxygen remained constant (within experimental error) both in the dark and during illumination, demonstrating a fairly good air-conditioning of the cell suspension through thin wall of plastic tube. In case of an oxygen-impermeable quartz cuvette, we observed the consumption of oxygen in the dark and its transient recovery during illumination (Fig. 9). A characteristic delay in the kinetics of P700 oxidation in response to switching-on the light after a dark pause correlates with an explicit lag-phase in the kinetics of the oxygen evolution (see inset in Fig. 9). Such a correlation between the light-induced evolution of oxygen and oxidation of P700 clearly demonstrates that photosynthetic electron transport is controlled by oxygen concentration in cell suspension. Note that the oxygen concentration in the WT sample first increased with illumination and then decreased. We think that this effect might be caused by photoinhibition of PS II (after 10-min illumination with white light).

4. Discussion

In this work, by using the EPR spectroscopy technique we investigated the light-induced redox transients of P700 and oxygen exchange processes under similar experimental conditions in intact cells of the cyanobacterium *Synechocystis* sp. PCC 6803. The rates of electron transfer through photosynthetic and respiratory electron transport chains depend on energization of the thylakoid membrane and oxygenation of cell suspension. The kinetic behavior of the EPR signal from oxidized centers $P700^+$ depends on the time of dark adaptation prior to illumination and conditions of cell incubation (gas permeable tube or quartz cuvette). The multiphase kinetics of P700 photo-oxidation in dark-adapted cells reflects the light-induced changes in the rates of electron transport on the donor and acceptor sides of PS I and may be conditioned by the following mechanisms:

(i) Acceleration of electron efflux from PS I due to regeneration of oxygen in de-aerated cell suspension, which promotes pseudocyclic electron flow, and/or activation of the Calvin cycle reactions;
(ii) Redistribution of electron fluxes between different pathways of electron transport, which may include switching between photosynthetic (noncyclic and cyclic) and respiratory electron transport chains;
(iii) Slowing down of electron donation from PQH_2 to $P700^+$ (via cyt *bf*-complex and plastocyanin) caused by acidification of the intrathylakoid lumen.

Oxygenation of cell suspension was shown to be an essential factor of electron transport control in *Synechocystis* sp. PCC 6803. Significant influence of oxygen on the light-

induced redox transients of P700 (Figs. 2 and 3) can be explained by several reasons. First, relatively low level of $P700^+$ observed during illumination of de-aerated cells (<10–20% of normal oxygen concentration) may indicate that the efflux of electrons from PS I is the rate-limiting step in the linear electron transport chain. According to Ref. [24], the addition of an artificial electron acceptor for PS I, methyl viologen, stimulates the rate of P700 photo-oxidation in de-aerated cells. Second, in line with the data obtained in [38,39], we suggest that at low concentrations of oxygen, when pseudocyclic "water→water" electron flow (H_2O→PS II→PS I→O_2→H_2O) [40,41] is diminished, electrons from PS I are re-directed, at least partly, to cyclic pathway around PS I. Therefore, in de-aerated cells concentration of $P700^+$ is maintained at a rather low level. Thus, under conditions of oxygen deficiency, cyanobacteria might retain their photosynthetic activity due to cyclic electron transport. Note that cyclic pathways may include the 'long' and 'short' routes. The 'long pathway' involves the NDH-1 complex: PS I→Fd→NADPH→NDH-1→PQH_2→cyt *bf*-complex→cyt c_6/Pc→$P700^+$ [42–45]. The 'short pathway' does not depend on NDH-1 activity: PS I→Fd→PQH_2→cyt *bf*-complex→cyt c_6/Pc→$P700^+$ [11,12]. In higher plant chloroplasts, the 'short pathway' is mediated by the PGR5 (proton gradient regulating) protein [46,47]. Under the oxygen deficiency conditions, cyclic electron transport can sustain the ATP synthesis, providing thereby the normal functioning of the Calvin cycle [10] and ATP-dependent carbon concentrating mechanisms [13].

Effects of oxygen depletion on the kinetics of P700 redox transients (Figs. 2 and 3) can also be explained by oxygen-dependent redistribution of electron fluxes between photosynthetic and respiratory chains. In cyanobacteria, these chains share common electron carriers, including the plastoquinone pool and the cyt *bf*-complex. In aerated suspension of cells, the terminal oxidases compete with $P700^+$ for electrons from plastoquinol (PQH_2→cyt *bd*→O_2) and cyt c_6 (cyt c_6→cyt aa_3→O_2), thus decreasing the electron flux to $P700^+$ (PQH_2→cyt *bf*→plastocyanin/cyt c_6→$P700^+$). When oxygen concentration goes down, the pool of electron carriers between two photosystems becomes over-reduced, leading to a decrease in the level of $P700^+$.

Oxygenation of cells facilitates the efflux of electrons from PS I, promoting the elevation of $P700^+$ level during illumination. This is because oxygen acts as the electron acceptor, which prevents the over-reduction of electron carriers on the acceptor side of PS I [41]. We demonstrated a correlation between the light-induced evolution of oxygen by PS II and photo-oxidation of P700 (Fig. 9). Under aerobic conditions, when the acceptor side of PS I imposes no limitation on the efflux of electrons from PS I, we evaluated the relative contribution of PS II to the electron flux to $P700^+$ as 70–80%, whereas remaining 20–30% of electrons available for $P700^+$ came from the dehydrogenases of the respiratory chains and cyclic electron transport. According to Refs. [16,17,48], the electron transfer capacities of oxidases in cyanobacteria are about 10% relative to photosynthetic electron transfer.

Another factor of the light-induced regulation of electron transport in cyanobacteria is the feedback control of electron flow governed by the intrathylakoid pH (pH_{in}). In chloroplasts, the rate-limiting step in the chain of electron transfer between two photosystems is the oxidation of PQH_2 by cyt *bf*-complex, which is controlled by pH_{in} [5–8]. Photosynthetic and respiratory electron transport chains in cyanobacteria share common electron carriers, including the plastoquinone pool and the cyt *bf*-complex. Similarly to higher plant chloroplasts [5–8], acidification of the intrathylakoid lumen in cyanobacteria can also cause the slowing down of PQH_2 oxidation by cyt *bf*-complex. Indeed, the protonophore uncoupler CCCP, which dissipates the transmembrane proton gradient, accelerates both the rate of electron flow to $P700^+$ and the rate of respiration (Fig. 4). Earlier [24], comparing the influence of nigericin and valinomycin on the kinetics of P700 redox transients, we came to the conclusion that generation of the transmembrane pH difference, which is associated with accumulation of protons in the intrathylakoid lumen, rather than generation of the transmembrane electric potential difference ($\Delta\psi$) was a dominant factor of slowing down the photosynthetic electron transport in *Synechocystis* sp. PCC 6803. Comparative study of the effects of nigericin and valinomycin on the respiration rate, carried out using the oxygen sensitive spin label TCPO (data not shown), demonstrated that respiration was controlled predominantly by the concentration component of $\Delta\mu_{H^+}$. Other possible mechanisms of the light-induced stimulation of electron transport in cyanobacteria may include: (i) $\Delta\mu_{H^+}$-dependent and/or ATP-dependent activation of CO_2 concentrating systems [13], (ii) $\Delta\mu_{H^+}$-dependent activation of ATP synthase [49], and (iii) thioredoxin-mediated activation of the Calvin cycle enzymes [9].

5. Conclusions

By using EPR spectroscopy to investigate electron transport through the PS I reaction center and oxygen exchange processes, we demonstrated that photosynthetic electron transport in *Synechocystis* sp. PCC 6803 was regulated both on the donor and on the acceptor sides of PS I. We conclude that photosynthetic electron transport through PS I is controlled by two main mechanisms: (i) oxygen-dependent acceleration of electron efflux from PS I, and (ii) modulation of the rate of electron transfer to PS I. Photosynthetic electron transport strongly depends on the presence of oxygen in cell suspension; in de-aerated cells the efflux of electrons from PS I becomes the rate-limiting step. We assume, however, that de-aerated cyanobacteria could retain high photosynthetic activity by directing electrons from PS I to the cyclic electron transport chains.

Electron fluxes from dehydrogenases and from cyclic electron transport pathway constitute 20–30% of the total electron flux from the intersystem electron transport chain to $P700^+$. The light-induced energization of thylakoid membranes leads to stimulation of electron efflux from PS I (likely due to activation of the Calvin cycle enzymes) and causes the slowing down of the electron transport between two photosystems. Further research will be focused on the quantitative determination of the proton gradient across the thylakoid membrane with pH-sensitive spin probes [35,50] in cyanobacteria functioning under different metabolic conditions.

Acknowledgments

This work was supported by Grants 99-1086 and 01-483 from the INTAS, Grants from the Russian Foundation for Basic Researches (03-04-48981, 03-04-48983, 04-04-49441, and 04-04-49332), Grant 2296 from the International Science and Technology Center (ISTC), Grant RC1-2400-MO-02 from the Civilian Research and Development Foundation (CRDF), Program "Russian Universities" (Grant 01.03.081) and Grant for Biophotonics Research from the Moscow State University. We thank Dr. W. Vermaas for gift of mutant cells and Dr. S. Chamorovsky for critical reading the manuscript.

References

[1] R.E. Blankenship, Molecular Mechanisms of Photosynthesis, Blackwell Science, 2002.
[2] G. Noctor, C.H. Foyer, Homeostasis of adenylate status during photosynthesis in a fluctuating environment, J. Exp. Bot. 51 (2000) 347–356.
[3] A.R. Grossman, D. Bhaya, Q. He, Tracking the light environment by cyanobacteria and the dynamic nature by light harvesting, J. Biol. Chem. 276 (2001) 11449–11452.
[4] A. Haldrup, P.E. Jensen, C. Lunde, H.V. Scheller, Balance of power: a view of the mechanism of photosynthetic state transitions, Trends Plant Sci. 6 (2001) 301–305.
[5] B. Rumberg, U. Siggel, pH changes in the inner phase of the thylakoid during photosynthesis, Naturwissenschaften 56 (1969) 130–132.
[6] A.N. Tikhonov, G.B. Khomutov, E.K. Ruuge, L.A. Blumenfeld, Electron transport control in chloroplasts. Effects of photosynthetic control monitored by the intrathylakoid pH, Biochim. Biophys. Acta 637 (1981) 321–333.
[7] L.A. Blumenfeld, A.N. Tikhonov, Biophysical Thermodynamics of Intracellular Processes, Molecular Machines of the Living Cell, Springer-Verlag, New York, 1994.
[8] D.M. Kramer, C.A. Sacksteder, J.A. Cruz, How acidic is the lumen? Photosynth. Res. 60 (1999) 151–163.
[9] B.B. Buchanan, Regulation of CO_2 assimilation in oxygenic photosynthesis: the ferredoxin/thioredoxin system. Perspective on its discovery, present status, and future development, Arch. Biochem. Biophys. 288 (1991) 1–9.
[10] J.F. Allen, State transitions—A question of balance, Science 299 (2003) 1530–1532.
[11] D.S. Bendall, R.S. Manasse, Cyclic photophosorylation and electron transport, Biochim. Biophys. Acta 1229 (1995) 23–38.
[12] P. Joliot, A. Joliot, Cyclic electron transfer in plant leaf, Proc. Natl. Acad. Sci. U. S. A. 99 (2002) 10209–10214.
[13] M.R. Badger, G.D. Price, CO_2 concentrating mechanisms in cyanobacteria: molecular components, their diversity and evolution, J. Exp. Bot. 54 (2003) 609–622.
[14] T. Pfannschmidt, Chloroplast redox signals: low photosynthesis controls its own genes, Trends Plant Sci. 8 (2003) 33–41.
[15] R. van Lis, A. Atteia, Control of mitochondrial function via photosynthetic redox signals, Photosynth. Res. 79 (2004) 133–148.
[16] G.A. Peschek, Respiratory electron transport, in: P. Fay, C. Van Baalen (Eds.), The Cyanobacteria, Elsevier, Amsterdam, The Netherlands, 1987, pp. 119–161.
[17] G. Schmetterer, Cyanobacterial respiration, in: D.A. Bryant (Ed.), The Molecular Biology of Cyanobacteria, Kluwer, Dordrecht, The Netherlands, 1994, pp. 409–435.
[18] T. Kaneko, S. Sato, A. Kotani, A. Tanaka, E. Asamizu, Y. Nakamura, N. Miyajima, M. Hirosawa, M. Sugiura, S. Sasamoto, T. Kimura, T. Hosochi, A. Matsuno, A. Muraki, N. Nakazaki, K. Naruo, S. Okamura, S. Shimpo, C. Takenchi, T.T. Wada, A. Watanabe, M. Yamada, M. Yasuda, S. Tabata, Sequence analysis of the genome of the unicellular cyanobacterium *Synechocystis* sp. strain PCC6803: II. Sequence determination of the entire genome and assignment of potential protein-coding regions, DNA Res. 3 (1996) 109–136.
[19] A. Zouni, H.-T. Witt, J. Kern, P. Fromme, N. Krauβ, W. Saenger, P. Orth, Crystal structure of photosystem II from Synechococcus elongatus at 3.8 A resolution, Nature 409 (2001) 739–743.
[20] P. Jordan, P. Fromme, H.-T. Witt, O. Klukas, W. Saenger, N. Krauβ, Three-dimensional structure of cyanobacterial photosystem I at 2.5 A resolution, Nature 411 (2001) 909–917.
[21] G. Kurisu, H. Zhang, J.L. Smith, W.A. Cramer, Structure of the cytochrome bf complex of oxygenic photosynthesis: tuning the cavity, Science 302 (2003) 1009–1014.
[22] A. Ben-Shem, F. Frolow, N. Nelson, Crystal structure of plant photosystem I, Nature 426 (2003) 630–635.
[23] N. Kamiya, J.-R. Shen, Crystal structure of oxygen-evolving photosystem II from Thermosynechococcus vulcanus at 3.7-A resolution, Proc. Natl. Acad. Sci. U. S. A. 100 (2003) 98–103.
[24] B.V. Trubitsin, M.D. Mamedov, L.A. Vitukhnovskaya, A.Yu. Semenov, A.N. Tikhonov, EPR study of light-induced regulation of photosynthetic electron transport in photosystem I complexes, FEBS Lett. 544 (2003) 15–20.
[25] R. Rippka, J. Derulles, J.B. Waterbury, M. Herdman, R.Y. Stanier, Genetic assignments, strain histories and properties of pure cultures of cyanobacteria, J. Gen. Microbiol. 181 (1979) 1–60.
[26] C.A. Howitt, W.F.J. Vermaas, Quinol and cytochrome oxidases in the cyanobacterium *Synechocystis* sp. PCC 6803, Biochemistry 37 (1998) 17944–17951.
[27] C.A. Howitt, J.W. Cooley, J.T. Wiskich, W.F.J. Vermaas, A strain of *Synechocystis* sp. PCC 6803 without photosynthetic oxygen evolution and respiratory oxygen consumption: implications for the study of cyclic photosynthetic electron transport, Planta 214 (2001) 46–56.
[28] G. Shen, J. Zhao, S.K. Reimer, M.L. Antonkine, Q. Cay, S.M. Weiland, G.H. Golbeck, D.A. Bryant, Assembly of photosystem I: I. Inactivation of the *rubA* gene encoding a membrane-associated rubredoxin in the cyanobacterium *Synechococcus* sp. PCC 7002 causes a loss of photosystem I activity, J. Biol. Chem. 277 (2002) 20343–20354.
[29] E.G. Rozantsev, L.A. Krinitskaya, Free iminoxyl radicals in the hydrogenated pyrrole series, Tetrahedron 21 (1965) 491–497.
[30] A.W. Rutherford, A. Boussac, P. Faller, The stable tyrosyl radical in photosystem II: why D? Biochim. Biophys. Acta 1655 (2004) 222–230.
[31] A.N. Webber, W. Lubitz, P700: the primary electron donor of photosystem I, Biochim. Biophys. Acta 1507 (2001) 61–79.
[32] G. Renger, Studies on the mechanism of the water oxidation in photosynthesis, Eur. J. Biochem. 27 (1972) 259–269.
[33] J.S. Hyde, W.K. Subczynski, Spin-label oximetry, in: L.J. Berliner, J. Rueben (Eds.), Biological Magnetic Resonance, Spin Labeling,

Theory and Applications, vol. 8, Plenum Press, New York, 1989, pp. 399–425.
[34] W.K. Subczynski, A. Cieslikowska, A.N. Tikhonov, Light-induced oxygen uptake in chloroplasts: ESR spin-label oximetry, Photosynthetica 24 (1990) 75–84.
[35] A.N. Tikhonov, W.K. Subczynski, Applications of spin labels to membrane bioenergetics (photosynthetic systems of higher plants), Chapter 8, in: S.S. Eaton, G.R. Eaton, L.J. Berliner (Eds.), Biological Magnetic Resonance, Biomedical EPR-Part A: Free Radicals, Metals, Medicine, and Physiology, vol. 23, Kluwer Academic/Plenum Publishers, New York, 2005, pp. 147–194.
[36] P. Bennoun, The present model for chlororespiration, Photosynth. Res. 73 (2002) 273–277.
[37] H.-B. Mao, G.-F. Li, D.-H. Li, Q.-Y. Wu, Y.-D. Gong, X.-F. Zhang, N.-M. Zhao, Effects of glycerol and high temperatures on structure and function of phycobilisomes in *Synechocystis* sp. PCC 6803, FEBS Lett. 553 (2003) 68–72.
[38] C.A. Howitt, J.W. Cooley, J.T. Wiskich, W.F.J. Vermaas, A strain of *Synechocystis* sp. PCC 6803 without photosynthetic oxygen evolution and respiratory oxygen consumption: implications for the study of cyclic photosynthetic electron transport, Planta 214 (2001) 46–56.
[39] S. Berry, D. Schneider, W.F.J. Vermaas, M. Rogner, Electron transport routes in whole cells of *Synechocystis* sp. strain PCC 6803: the role of the cytochrome bd-type oxidase, Biochemistry 41 (2002) 3422–3429.
[40] K. Asada, The water–water cycle in chloroplasts: scavenging of active oxygens and dissipation of excess photons, Annu. Rev. Plant Physiol. Plant Mol. Biol. 50 (1999) 601–639.
[41] J.E. Backhausen, C. Kitzmann, P. Horton, R. Scheibe, Electron acceptors in isolated intact spinach chloroplasts act hierarchically to prevent over-reduction and competition for electrons, Photosynth. Res. 64 (2000) 1–13.
[42] H. Mi, T. Endo, U. Schreiber, T. Ogawa, K. Asada, Electron donation from cyclic and respiratory flows to the photosynthetic intersystem chain is mediated by pyridine nucleotide dehydrogenase in the cyanobacterium *Synechocystis* PCC 6803, Plant Cell Physiol. 33 (1992) 1233–1237.
[43] H. Mi, T. Endo, T. Ogawa, K. Asada, Thylakoid membrane-bound, NADPH-specific pyridine nucleotide dehydrogenase complex mediates cyclic transport in the cyanobacterium *Synechocystis* sp. Strain PCC 6803, Plant Cell Physiol. 36 (1995) 661–668.
[44] P.A. Burrows, L.F. Sazanov, Z. Svab, P. Maliga, P.J. Nixon, Identification of a functional respiratory complex in chloroplasts through analysis of tobacco mutants containing disrupted plastid *ndh* genes, EMBO J. 17 (1998) 868–876.
[45] H. Mi, Y. Deng, Y. Tanaka, T. Hibino, T. Takabe, Photo-induction of an NADPH dehydrogenase which functions as a mediator of electron transport to the intersystem in the cyanobacterium *Synechocystis* PCC 6803, Photosynth. Res. 70 (2001) 167–173.
[46] Y. Munekage, M. Hojo, J. Meurer, T. Endo, M. Tasaka, T. Shikanai, PGR5 is involved in cyclic electron flow around photosystem I and is essential for photoprotection in *Arabidopsis*, Cell 110 (2002) 361–371.
[47] Y. Munekage, M. Hashimoto, C. Miyake, K.-I. Tomizawa, T. Endo, M. Tasaka, T. Shikanai, Cyclic electron flow around photosystem I is essential for photosynthesis, Nature 429 (2004) 579–582.
[48] L. Yu, J. Zhao, U. Muhlenhoff, D.A. Bryant, J.H. Golbeck, PsaE is required for in vivo cyclic electron flow around photosystem I in the cyanobacterium *Synechococcus* sp. PCC 7002, Plant Physiol. 103 (1993) 171–180.
[49] Y. Evron, E.A. Johnson, R.E. McCarty, Regulation of proton flow and ATP synthesis in chloroplasts, J. Bioenerg. Biomembranes 32 (2000) 501–506.
[50] B.V. Trubitsin, A.N. Tikhonov, Determination of a transmembrane pH difference in chloroplasts with a spin label tempamine, J. Magn. Res. 163 (2003) 257–269.